AFFDL-TR-68-150

FINITE ELEMENT ANALYSIS OF FLUID FLOWS

Harold C. Martin*
University of Washington

The finite element method is applied to several simple cases of steady flow of a perfect, incompressible fluid. It is shown that the finite element representation accurately reflects the behavior of the classical flow equations. Some finite element theory is included for the reader who may be unfamiliar with this subject.

*Professor, Department of Aeronautics and Astronautics

SECTION I

INTRODUCTION

Finite elements form the basis for a versatile analysis procedure applicable to problems in several different fields. Earliest applications were to problems in structural mechanics (Reference 1). In recent years non-structural problems have also been treated by this method (Reference 2).

Basically, the finite element method represents an approximate procedure for satisfying the problem in terms of its variational formulation. In structural mechanics, for example, this is generally accomplished by determining displacement fields based on satisfying the minimum potential energy theorem. Consequently, finite elements furnish a useful alternative scheme for applying the well-known Ritz method. In developing the method for nonstructural problems, it is essential that the appropriate variational expressions be known beforehand. For the flow problems taken up in this paper, such expressions are well known.

The area or volume defining the total region of a problem may be considered to be decomposed into an assemblage of subregions. For example, in the case of a two dimensional flow these subregions may be taken as triangles of arbitrary size and shape. Each such triangular region represents a finite element. Vertices of the triangles become nodal points of the finite element assemblage. They assume a particular importance in the development of the finite element equations. Figures 1 and 2 show typical assemblages based on the triangular element.

The governing matrix equation for the assemblage of elements is based on the properties derived for a single typical element. These properties, in turn, depend on assuming a mathematical form for the primary unknown of the problem and then satisfying the variational principle. For the elasticity problem, the unknowns are the displacements, while for the perfect incompressible fluid, either the velocity potential or the stream function may be used.

Of great interest is the fact that structural and nonstructural elements may often be identical in shape and, further, be represented by similar mathematical expressions. For example, the triangle in elasticity will have the same form for displacements u and v, as the similar fluid flow element has for velocity potential ϕ or stream function ψ. In addition, the numerical solution procedure will be quite similar for each case. By way of illustration, the

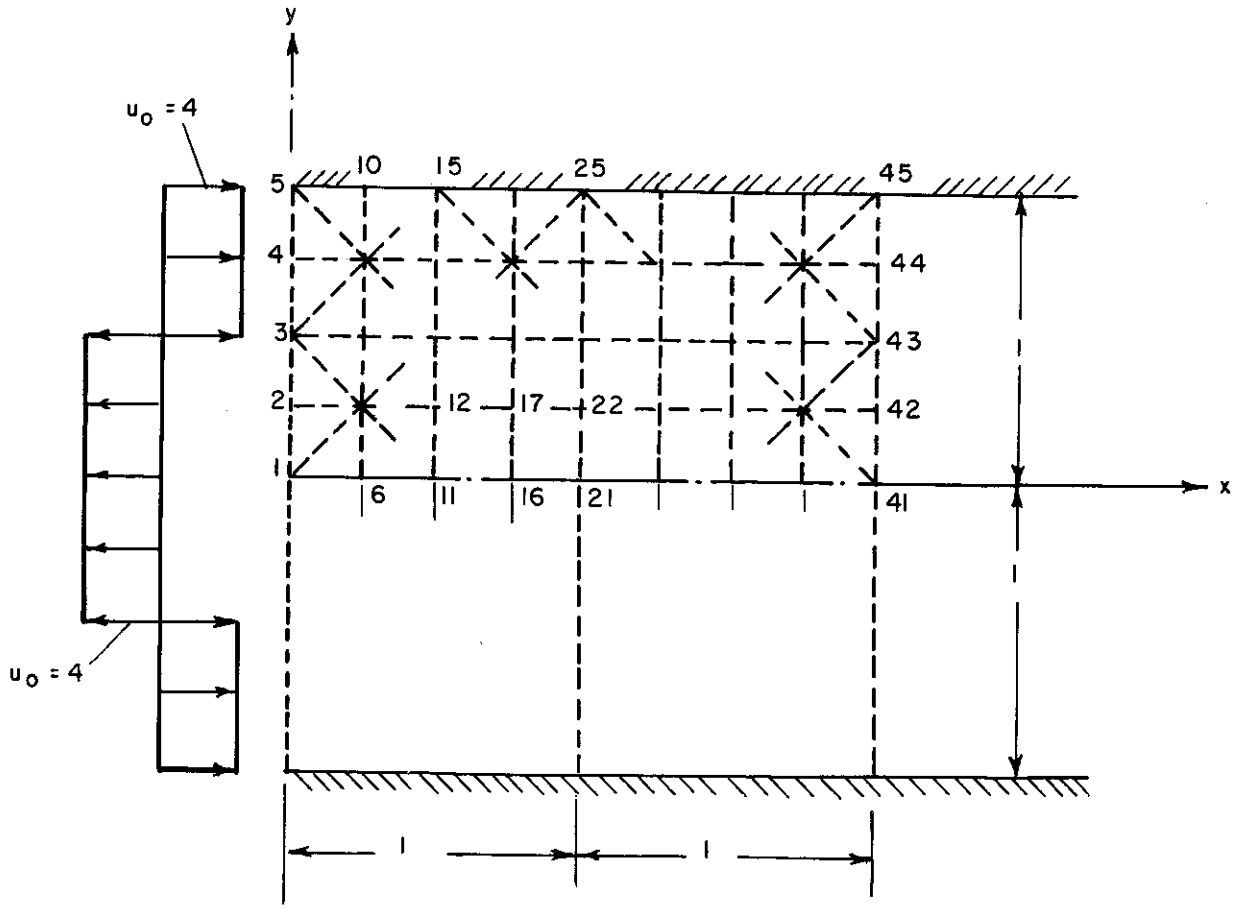

Figure 1. Saint Venant Flow Problem

problems taken up in this paper were solved using the new ASTRA structural program developed at The Boeing Company. This versatility, provided by finite elements and associated computer programs, is obviously of great practical importance.

Finally, it should be pointed out that the major difference between the elasticity and fluid flow problems lies in the boundary conditions to be satisfied. This question is therefore taken up in the paper.

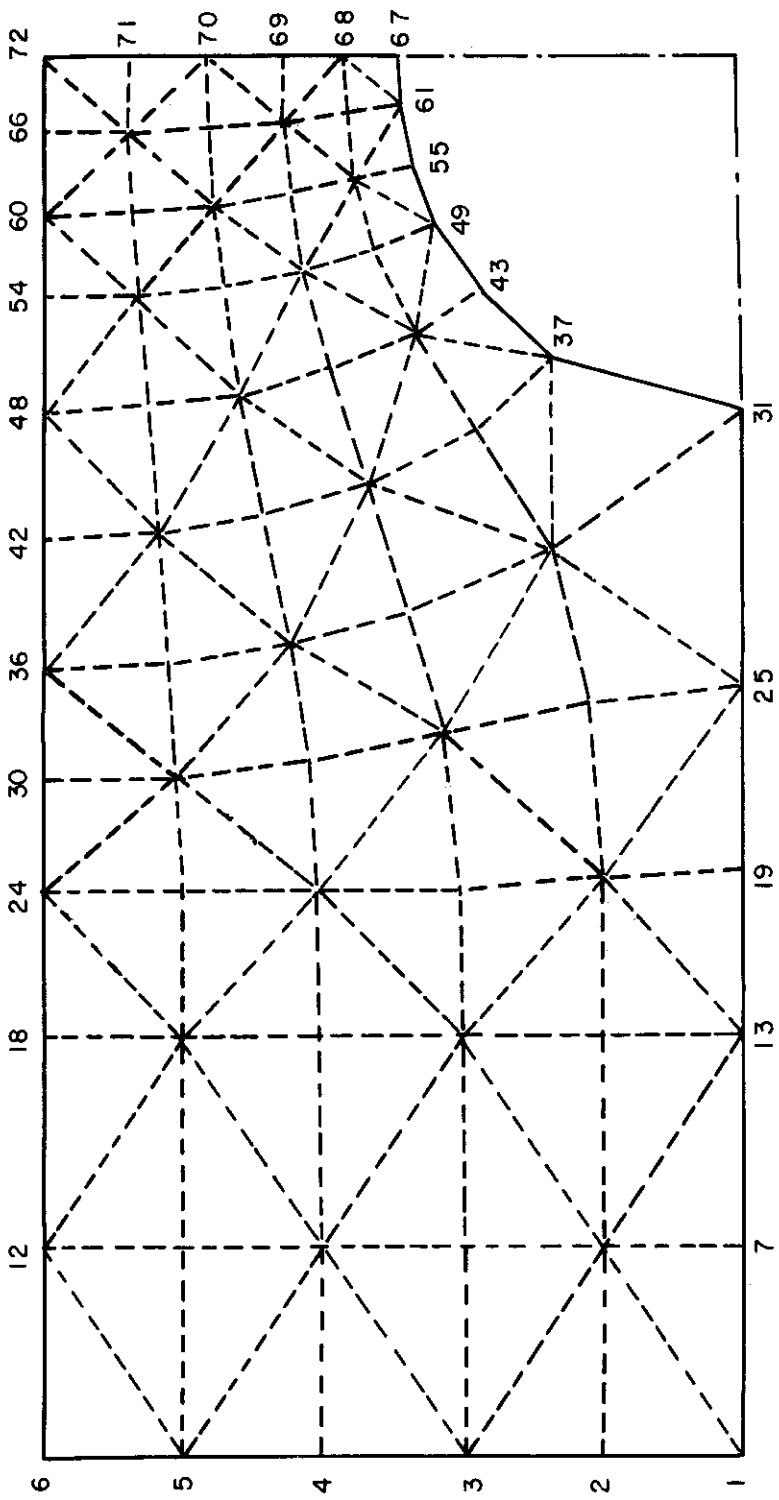

Figure 2. Finite Element Idealization of Cylinder Flow Problem

SECTION II

BASIC THEORY

Let u, v represent the velocity components in a two dimensional flow. Then in terms of velocity potential ϕ (x,y)

$$u = \frac{\partial \phi}{\partial x} \qquad v = \frac{\partial \phi}{\partial y} \tag{1}$$

while in terms of the stream function ψ (x,y)

$$u = \frac{\partial \psi}{\partial y} \qquad v = -\frac{\partial \psi}{\partial x} \tag{2}$$

Both ϕ and ψ must satisfy LaPlace's equation or,

$$\frac{\partial^2 ( )}{\partial x^2} + \frac{\partial^2 ( )}{\partial y^2} = 0 \tag{3}$$

As shown in variational calculus, LaPlace's equation may alternatively be expressed in terms of a minimum principle (Reference 3). The principle is as follows: that function which satisfies LaPlace's equation in a region R and which takes on prescribed values along the boundary of R, will have a mean square gradient which is a minimum over region R. Or,

$$\delta I = \delta \iint \frac{1}{2} \left\{ \left(\frac{\partial \psi}{\partial x} \right)^2 + \left(\frac{\partial \psi}{\partial y} \right)^2 \right\} \, dx dy = 0 \tag{4}$$

The equation also holds for velocity potential ϕ. Note that this is the Dirichlet problem in which ψ, rather than derivatives of ψ, are prescribed on the boundary.

On solid boundaries, values for ψ can be specified. At other points, as the left hand cross-section of Figures 1 or 5, the velocity is known and is given in terms of a derivative of ψ. Further attention must be given to such boundaries. In the case of ϕ, it is not known on solid walls or other bodies in the flow; however, the flow $\partial\phi/\partial n$ normal to such surfaces must be zero. In general then, it will be more difficult to treat the problem in terms of ϕ. These points are taken up in detail when the examples of Figures 1 and 5 are discussed.

That function ψ (x,y) which satisfies Equation 4, and the boundary conditions will be the solution to the problem. Such a function must have continuous second partial derivatives within each subregion of R and must be continuous on all element boundaries. The purpose will now be to find an approximate solution in terms of an assumed function ψ (x,y).

The assumed function is chosen with a single element in mind. Such an arbitrary triangle is shown in Figure 3. In selecting the function $\psi(x,y)$, the following points are kept in mind: (1) the function must be given in terms of x and y and the values which it has at the nodes (1, 2, 3 Figure 3); (2) continuity must exist in $\psi(x,y)$ at interfaces of adjoining elements; (3) velocities (Equation 2) must include constant terms. These conditions will not be discussed here. They are necessary in order to guarantee boundedness and convergence of the finite element solution. (References 4 and 5).

Based on the assumed form for $\psi(x,y)$, Equation 4 will be satisfied approximately by minimizing ψ with respect to its nodal values $\{\psi_i\}$. Or,

$$\frac{\partial I}{\partial \{\psi_i\}} = 0 \tag{5}$$

This will lead directly to the fluid element stiffness equation, which takes the form,

$$[k]\{\psi_i\} = \{0\} \tag{6}$$

where $[k]$ is the fluid element stiffness matrix. It will be symmetric and singular for structural elements.

This equation for the element may now be treated precisely for the structural case in forming the total assemblage stiffness equation; that, by a simple superposition procedure (Reference 1 or 2). Let this equation be given by,

$$[K]\{\psi\} = \{0\} \tag{7}$$

If ψ_a are unknown, while ψ_b are prescribed (the Dirichlet problem), Equation 7 may be written as,

$$\begin{bmatrix} K_{aa} & K_{ab} \\ K_{ab}^T & K_{bb} \end{bmatrix} \begin{bmatrix} \psi_a \\ \psi_b \end{bmatrix} = 0 \tag{8}$$

Then,

$$K_{aa}\ \psi_a + K_{ab}\ \psi_b = 0 \tag{9a}$$

$$K_{ab}^T\ \psi_a + K_{bb}\ \psi_b = 0 \tag{9b}$$

Since ψ_b is known, Equation 9a may be used to find ψ_a or,

$$\psi_a = -(K_{aa})^{-1}\ K_{ab}\ \psi_b \tag{10}$$

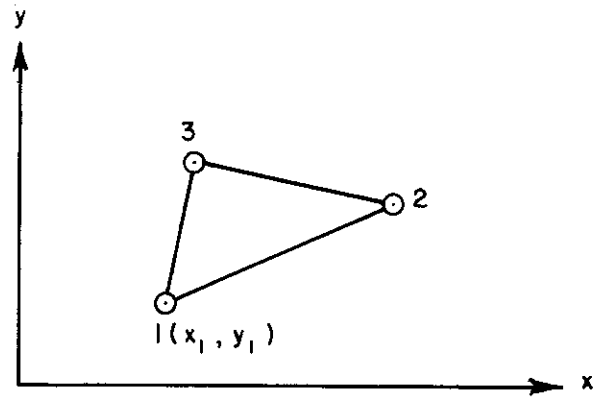

Figure 3. The Triangular Finite Element

Note that whereas $\mathbf{K}$ of Equation 7 is singular, the submatrix $\mathbf{K}_{aa}$ of Equation 9a will be nonsingular. Equation 9b cannot be used in finding ψ_a since $\mathbf{K}^T_{ab}$ need not be a square matrix and hence, cannot be inverted.

The derivation of the element stiffness matrix, Equation 6, is given in the Appendix.

SECTION III

SAINT VENANT'S PRINCIPLE IN FLUID FLOW

Saint Venant's principle, although widely known in solid mechanics, seems to be rather infrequently referred to in fluid mechanics. Nevertheless, this principle is investigated in Reference 6 for incompressible potential flows. It is shown that if the net mass flow at a given station in a channel is zero, the velocity profile will approach zero a short distance downstream. The analogy with the structural case is self-evident.

Figure 1 shows a typical flow to which St. Venant's principle must apply. The net flow entering the channel is zero; hence, the velocities should quickly approach zero as the fluid moves downstream. The flow may be taken as two dimensional.

Boundary conditions are as follows:

$$\psi = 0 \quad \text{on} \quad y = 0, \ 1 \tag{11}$$

$$u = u_0 \quad \text{on} \quad x = 0 \tag{12}$$

Due to symmetry, only the upper half of the channel need be considered.

The mixed boundary value problem represented by Equations 11 and 12 can be easily replaced by a Dirichlet type problem. To do this, it is merely necessary to use the definition of the stream function and thereby replace u on $x = 0$ with ψ. With Figure 1 in mind, it follows that,

$$\psi_2 = \psi_1 + u_0 y_{21} \quad \text{where} \quad y_{21} = y_2 - y_1$$
$$= 1$$

Similarly, it is found that $\psi_3 = 0$, $\psi_4 = -1$, and $\psi_5 = 0$. The result at node 5 agrees with the statement made in Equation 11. At a downstream boundary, say $x = 1$, ψ is unknown and hence, will be found as part of the solution.

The finite element representation is indicated in Figure 1. In terms of the triangular elements shown, the solution procedure follows the steps illustrated by Equations 8, 9, and 10. Results were obtained for ψ at the nodes and for velocity, u, for each element. Due to the linear form for ψ, and in view of Equation 2, it is seen that u can be also calculated from nodal values of the stream function.

Finite element results agree with Reference 6 and show that the St. Venant effect does indeed occur. Decay in the velocity profile depends only on x and was discovered to be independent of y. Therefore, results can be shown for the strip bounded by horizontal lines starting at nodes 1 and 2. Figure 4 shows the velocity decay for this strip. The curve applies equally well to the other similar strips.

It is interesting to note that the St. Venant effect occurs for the inviscid fluid. Hence, it reflects the intrinsic properties of governing fluid equations. These are seen to be reflected also by the finite element representation of the problem.

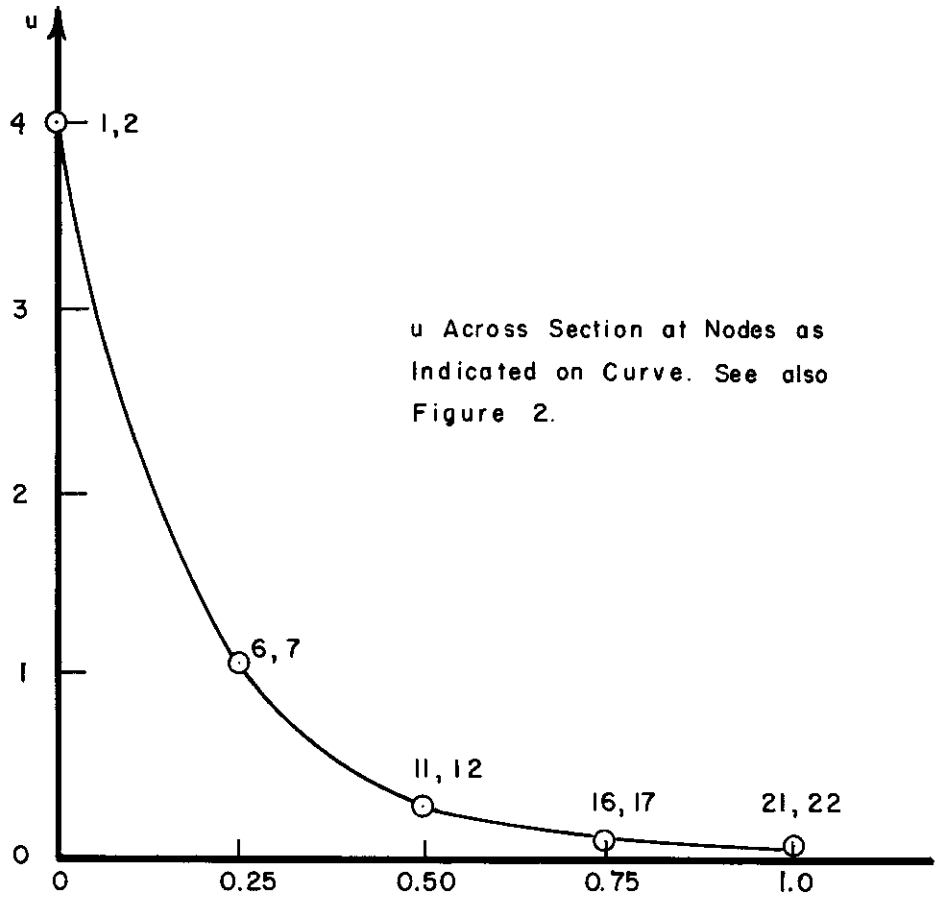

Figure 4. Velocity Decay for Saint Venant Flow

SECTION IV

FLOW AROUND CYLINDER BETWEEN PARALLEL WALLS

A simple, but nevertheless interesting boundary value problem is shown in Figure 5. Again the flow may be taken as two dimensional; furthermore, it is assumed that the flow is uniform at the upstream and downstream ends taken as shown in Figure 5.

An approximation to this problem is available in fluid theory (Reference 7). This is obtained by considering a distribution of doublets on a vertical line in the presence of a horizontal rectilinear flow. Unfortunately, this scheme yields a circular cylinder only when the strength of the doublets becomes small. As a result, the theoretical solution obtained in this manner does not fit the ratio of cylinder diameter to wall spacing shown in Figure 5. The author was unable to locate a theoretical solution valid for any ratio of cylinder diameter to wall spacing. It therefore may be appropriate to point out at this time that the finite element method is in no sense restricted to parallel walls or a circular cylinder.

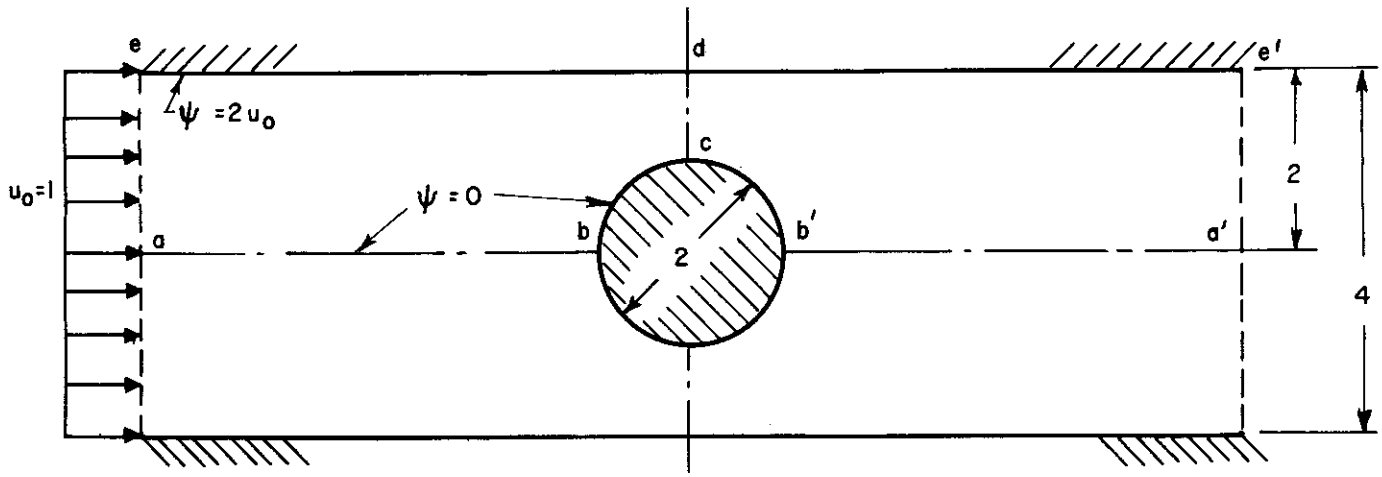

Figure 5. Flow Around Cylinder Between Parallel Walls

For the geometry shown in Figure 5, the solution based on the combination of doublets and flow u_0 gives

$$u_c = 2.33\ u_o \qquad u_d = 1.6\ u_o \tag{13}$$

These will be commented on later.

Boundary conditions depend on the region which will be considered in the finite element analysis. The smallest, and therefore most economical, region which can be used is a-b-c-d-e, as shown in Figure 5. Due to symmetry, it is again permissible to choose,

$$\psi = 0 \quad \text{along} \quad a-b \quad \text{and} \quad b-c \tag{14}$$

Then again, using the definition of the stream function,

$$\psi = 2 \quad \text{on} \quad d-e \tag{15}$$

Along a-e, values of ψ at nodal points can be specified in the same manner as used for the previous problem. Finally on c-d, the vertical component of velocity must vanish. This condition requires detailed attention, and this will be taken up subsequently. In the meantime, it is pointed out that the difficulty is by-passed if the total upper half of the flow field is considered. Boundary conditions on $a'e'$ are then the same as those on ae and the formulation becomes once again a Dirichlet type problem. This is the problem which was solved by finite elements.

The idealization of the flow field into a finite element representation is shown in Figure 2. Reflection of this pattern in the computer program established the right hand side of the flow field. Of interest is the fact that this same idealization had been previously used for analyzing the corresponding flat sheet with a circular cut-out. Therefore, considerable input data was already available for undertaking the fluid flow problem.

Again the computer furnished unknown values of ψ and the flow velocity in each triangular element. As a result, a complete picture of the flow field is therefore made available. Of maximum interest is the velocity distribution along c-d, Figure 5. This was calculated directly from the nodal values of ψ. These values are listed in Table 1. In addition, the y-coordinates of nodes lying on c-d are listed in this same table.

TABLE 1

Node	y-Coordinate	ψ
67	1.00	0
68	1.16	0.3419
69	1.33	0.6880
70	1.54	1.1072
71	1.76	1.5364
72	2.00	2.0000

For the point midway between nodes 67 and 68, the velocity is calculated as,

$$u_{67-68} = \frac{\psi_{68} - \psi_{67}}{y_{68} - y_{67}} = 2.20$$

Similarly for mid-points between the other nodes on c-d. These velocities are plotted in Figure 6. Extrapolation then gives velocity at the cylinder and on the wall as follows:

$$u_c = 2.20\ u_o \qquad u_d = 1.90\ u_o \tag{16}$$

These results can now be compared with those previously given in Equation 13.

As seen, results compare well at point c on the cylinder. Considerable discrepancy, however, exists at point d on the wall. The finite element result for u_d is undoubtedly close to the true value since from Figure 6, it is seen that it fits the velocity profile which will provide for continuity of the flow across line c-d (average velocity must be 2 at this section).

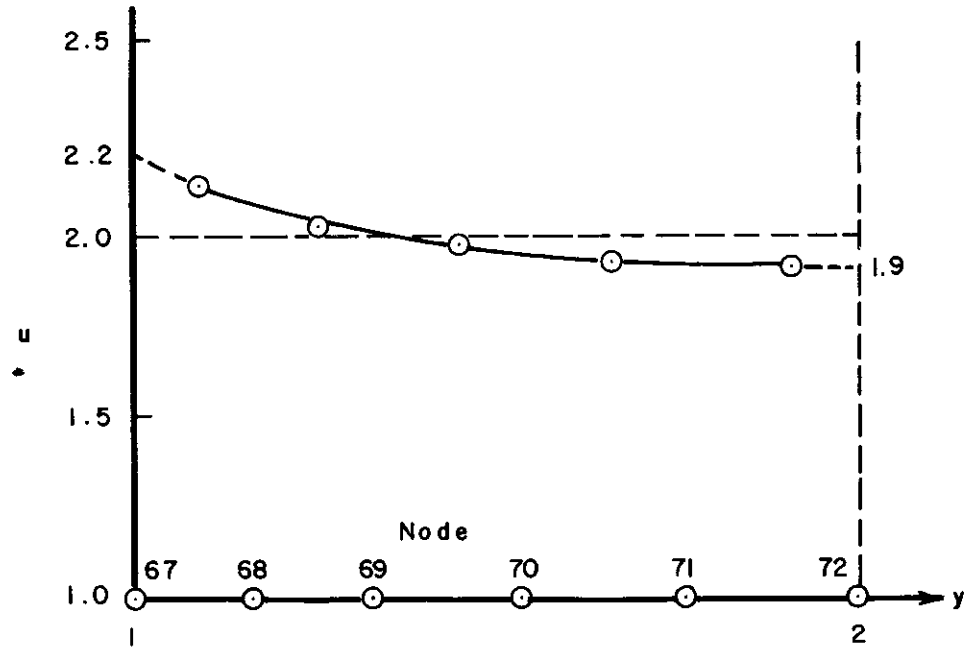

Figure 6. Velocity at Vertical Centerline (c-d, Figure 4)

SECTION V

BOUNDARY CONDITIONS OF THE NEUMANN TYPE

As seen in the preceding problem, it may be useful to prescribe boundary conditions which are given as derivatives of ψ. Generally, these would be prescribed on some boundaries, while ψ is prescribed on others. This mixed type boundary value problem causes no difficulty in itself, provided a scheme can be found for specifying boundary conditions associated with first derivatives of ψ. Furthermore, the procedure developed for handling such cases will then be directly applicable to flow problems formulated in terms of the velocity potential ϕ. In this latter case, however, since all boundary conditions would be written in terms of $\partial\phi/\partial n$, a further step is required in order to remove the singularity present in the stiffness matrix. As is well known, the solution to the Neumann type problem gives the potential function to the extent of an arbitrary constant. Therefore, in the flow problem given in terms of ϕ, it is permissible to arbitrarily select ϕ at one node (say $\phi = 0$ at a selected node). Imposing this condition on the stiffness equation for the assemblage will then remove the singularity in $\left[K\right]$. At this point, the boundary conditions in terms of $\partial\phi/\partial n$ must be specified. Hence, for the fluid problem, whether formulated in terms of ψ or ϕ, the Neumann type boundary condition needs to be considered. Similar situations do arise in some structural problems but they have only received scant attention.

Returning to the cylinder problem, consider again the situation along boundary c-d. Since v equals zero at this line, Equation 2 requires that,

$$v = -\frac{\partial\psi}{\partial x} = 0 \qquad \text{on} \qquad c-d \tag{17}$$

Two choices are available for imposing this condition on the problem. First, the element derivation which is given in the Appendix can be carried out with the restriction that $\partial\psi/\partial x$ be equal to zero. This will give an alternate form for the element stiffness matrix which can then be used for elements having nodes on c-d. The disadvantage is, of course, that such elements must then be incorporated into the computer program and used as need arises. In addition, versatility is lost in that a condition such as $\partial\phi/\partial n = 0$ on the cylinder is not easily imposed in this manner. Nevertheless, for certain special situations it may be useful to have such an element in the computer program.

The second possibility is to consider the boundary conditions on the velocity as constraints on the set of equations expressed as the gross assemblage stiffness equation. Imposing these constraints is then equivalent to a coordinate transformation in which the original set of nodal

values for ψ are replaced by a new set of generalized values ψ^*. In carrying out this transformation, it must be kept in mind that ψ (or ϕ) is a scalar and not a vector.

For simplicity, the element will be discussed rather than the assemblage. The treatment is essentially the same in each instance since the element stiffness equation is similar in form to the corresponding equation for the total assemblage. Also, the development will be carried out in terms of ψ although it can just as easily be written in terms of ϕ.

From Figure 7 it is seen that,

$$v_n = \frac{\partial \phi}{\partial n} = \lambda u + \mu v$$

and putting this equal to zero,

$$v_n = \lambda \frac{\partial \psi}{\partial y} - \mu \frac{\partial \psi}{\partial x} = 0 \tag{18}$$

From the development of $\psi(x,y)$ as given in the Appendix, it can be shown that,

$$\frac{\partial \psi}{\partial x} = \frac{1}{2A}(y_{23}\,\psi_1 + y_{31}\,\psi_2 + y_{12}\,\psi_3)$$

and,

$$\frac{\partial \psi}{\partial y} = \frac{1}{2A}(x_{32}\,\psi_1 + x_{13}\,\psi_2 + x_{21}\,\psi_3)$$

Substituting into Equation 18

$$(-\lambda y_{23} + \mu x_{32})\psi_1 + (-\lambda y_{31} + \mu x_{13})\psi_2 + (-\lambda y_{12} + \mu x_{21})\psi_3 = 0$$

Solving for ψ_2 in terms of ψ_1 and ψ_3, enables the following equation to be written,

$$\begin{bmatrix} \psi_1 \\ \psi_2 \\ \psi_3 \end{bmatrix} = \begin{bmatrix} 1 & 0 \\ \dfrac{\lambda y_{23} - \mu x_{32}}{-\lambda y_{31} + \mu x_{13}} & \dfrac{\lambda y_{12} - \mu x_{21}}{-\lambda y_{31} + \mu x_{13}} \\ 0 & 1 \end{bmatrix} \begin{bmatrix} \psi_1 \\ \\ \psi_3 \end{bmatrix} \tag{19}$$

or,

$$\{\psi_i\} = [A]\{\psi^*\} \tag{20}$$

Integral I of the variational equation may be written in terms of $[K]$ and $\{\psi_i\}$ as follows from the Appendix. Or,

$$I = \frac{1}{2}\{\psi_i\}^T [K]\{\psi_i\}$$

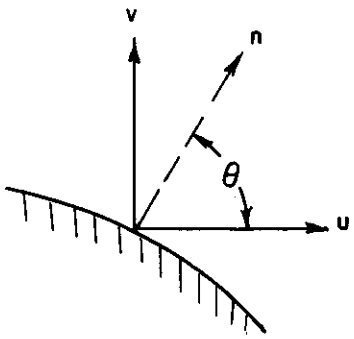

Figure 7. Velocities at Solid Boundary

Substituting from Equation 20 gives,

$$I = \frac{1}{2}\left\{\psi^*\right\}^T\left(\left[A\right]^T\left[K\right]\left[A\right]\right)\left\{\psi^*\right\} = \frac{1}{2}\left\{\psi^*\right\}\left[K^*\right]\left\{\psi^*\right\} \tag{21}$$

Equation 21 provides the stiffness matrix K*, subject to the condition $\partial\phi/\partial n = 0$. It was obtained by using the transformation expressed by Equations 19 and 20. Since these transformation equations can be written for all elements having nodes on the boundary where $\partial\phi/\partial n$ is to be prescribed, the treatment is applicable to the gross stiffness equation. The solution then gives $\left\{\psi^*\right\}$, from which the original values $\left\{\psi_i\right\}$ can be obtained from Equation 20.

The scheme outlined above was not used in solving the cylinder problem since it was not available in the ASTRA program at the time the solution was carried out.

SECTION VI

DISCUSSION

Analysis of fluid problems by finite elements has barely begun. It is expected that this subject will receive intensive development in the immediate future. Of great value for solving problems will be available structural elements and associated computer programs. These will permit analysis of two or three dimensional problems. Extension to more complex classes of fluid flow can also be expected.

Advantages of the finite element method over other numerical procedures has been well established in the existing literature (Reference 2).

Acknowledgements

The writer is indebted to B. E. Greene and J. L. White, of The Boeing Company, for useful discussion and comments. Also, appreciation is expressed to M. W. Ice and E. D. Herness for carrying out the solutions to the problems. This was done using the ASTRA finite element program, recently developed at The Boeing Company.

SECTION VII

REFERENCES

1. Turner, M. J. Clough, R. W., Martin, H. C., and Topp, L. J., "Stiffness and Deflection Analysis of Complex Structures," Journal of the Aeronautical Sciences, Vol. 23, No. 9, September 1956, pp. 805-824.

2. Zienkiewicz, O. C. and Cheung, Y. K., The Finite Element Method in Structural and Continuum Mechanics, McGraw-Hill Publishing Co., Ltd., 1967.

3. Hildebrand, F. B., "Methods of Applied Mathematics," Prentice-Hall, Inc., New York, 1952, p. 138.

4. Johnson, M. W. Jr. and McLay, R. W., "Convergence of the Finite Element Method in the Theory of Elasticity," accepted for publication in the ASME Journal of Applied Mechanics.

5. Felippa, C. A. and Clough, R. W., "The Finite Element Method in Solid Mechanics," presented at the Symposium on Numerical Solutions of Field Problems in Continuum Mechanics, Durham, North Carolina, April 5-6, 1968.

6. Drake, R. L. and Chou, P. C., "Upper Bounds and Saint Venant's Principle for Incompressible Potential-Flow Fields," Journal of Applied Mechanics, Transactions of the American Society of Mechanical Engineers, September 1965, pp. 661-664.

7. Streeter, V. L., "Fluid Dynamics," McGraw-Hill Book Company, 1948, pp. 116-119.

APPENDIX

The conditions as previously set forth for choosing $\psi(x,y)$ are met, in the case of the triangle, by taking

$$\psi(x,y) = \begin{bmatrix} 1 & x & y \end{bmatrix} \begin{bmatrix} a_0 \\ a_1 \\ a_2 \end{bmatrix} = \begin{bmatrix} f(x,y) \end{bmatrix} \{\alpha\} \tag{22}$$

Writing nodal values of ψ gives,

$$\begin{bmatrix} \psi_1 \\ \psi_2 \\ \psi_3 \end{bmatrix} = \begin{bmatrix} 1 & x_1 & y_1 \\ 1 & x_2 & y_2 \\ 1 & x_3 & y_3 \end{bmatrix} \{\alpha\}$$

or,

$$\{\psi_i\} = [L]\{\alpha\} \tag{23}$$

Substituting from Equation 23 into 22,

$$\psi(x,y) = \begin{bmatrix} f(x,y) \end{bmatrix} [L]^{-1} \{\psi_i\} \tag{24}$$

Equation 24 gives ψ in terms of its nodal values, ψ_i. Also note that since $\psi(x,y)$ is linear, it must be identical for adjoining elements A and B on common edge i-j. Hence, continuity in ψ along element interfaces is assured. From Equation 24,

$$\frac{\partial \psi}{\partial x} = \left[\frac{\partial f}{\partial x}\right][L]^{-1} \{\psi_i\} \tag{25}$$

and therefore,

$$\left(\frac{\partial \psi}{\partial x}\right)^2 = \{\psi_i\}^T \left([L]^{-1}\right)^T \left[\frac{\partial f}{\partial x}\right]^T \left[\frac{\partial f}{\partial x}\right][L]^{-1} \{\psi_i\}$$

A similar expression holds for $\left(\frac{\partial \psi}{\partial y}\right)^2$

Since $\left(\frac{\partial \psi}{\partial x}\right)^2$ is independent of x and y, and similarly for $\left(\frac{\partial \psi}{\partial y}\right)^2$, the integrand of Equation 4 will be constant.

Therefore,

$$I = \frac{A}{2} \{\psi_i\}^T \left([L]^{-1}\right)^T \left(\left[\frac{\partial f}{\partial x}\right]^T \left[\frac{\partial f}{\partial x}\right] + \left[\frac{\partial f}{\partial y}\right]^T \left[\frac{\partial f}{\partial y}\right]\right) [L]^{-1} \{\psi_i\}$$

where A is the area of the triangular element. Since I is quadratic in ψ_i, applying Equation 5 gives,

$$\frac{\partial I}{\partial \{\psi_i\}} = \left(\left[L\right]^{-1}\right)^T \left(\left[\frac{\partial f}{\partial x}\right]^T \left[\frac{\partial f}{\partial x}\right] + \left[\frac{\partial f}{\partial y}\right]^T \left[\frac{\partial f}{\partial y}\right]\right) \left[L\right]^{-1} \{\psi_i\} = 0 \tag{26}$$

or,

$$\left[K\right]\{\psi_i\} = \{0\} \tag{27}$$

where,

$$\left[K\right] = \frac{1}{4A} \begin{bmatrix} x_{32}^2 + y_{23}^2 & & \text{(SYMMETRIC)} \\ x_{13}\,x_{32} + y_{23}\,y_{31} & x_{13}^2 + y_{31}^2 & \\ x_{21}\,x_{32} + y_{12}\,y_{23} & x_{21}\,x_{13} + y_{12}\,y_{31} & x_{21}^2 + y_{12}^2 \end{bmatrix} \tag{28}$$

In this last equation, $x_{32} = x_3 - x_2$, etc.

The fluid element stiffness matrix, Equation 28, also appears as a submatrix in the corresponding structural element stiffness matrix. It is, therefore, possible to generate $\left[K\right]$ of Equation 28 from appropriate structural computer programs.